Chemical Engineering Journal 157 (2010) 579–589

Contents lists available at ScienceDirect

Chemical Engineering Journal

journal homepage: www.elsevier.com/locate/cej

Xylene isomerization kinetic over acid-functionalized silicalite-1 catalytic membranes: Experimental and modeling studies

Yin Fong Yeong, Ahmad Zuhairi Abdullah, Abdul Latif Ahmad, Subhash Bhatia*

School of Chemical Engineering, Engineering Campus, Universiti Sains Malaysia, Seri Ampangan, 14300 Nibong Tebal, Seberang Perai Selatan, Pulau, Pinang, Malaysia

ARTICLE INFO

Article history:
Received 7 October 2009
Received in revised form
25 December 2009
Accepted 11 January 2010

Keywords:
Synthesis
Acid-functionalized silicalite-1 membrane
m-Xylene isomerization
Catalytic activity
Kinetic modeling
Activation energy

ABSTRACT

m-Xylene isomerization kinetics has been studied using acid-functionalized silicalite-1 catalytic membrane in the temperature range of 355–450 °C. Two types of catalytic membranes: (1) propylsulfonic acid-functionalized silicalite-1 membrane and (2) arenesulfonic acid-functionalized silicalite-1 membrane were synthesized on α-alumina support via one-step *in situ* hydrothermal crystallization and subsequent post-synthesis modifications. The membranes were characterized by scanning electron microscopy (SEM), ammonia temperature-programmed desorption (NH_3-TPD) and Fourier transform infrared spectroscopy (FT-IR). Arenesulfonic acid-functionalized silicalite-1 membrane with its higher acidity gave better catalytic activity as compared to propylsulfonic acid-functionalized silicalite-1 membrane. The continuous removal of reaction products over the membrane contributed in the higher *p*-xylene yield. A triangular reaction scheme based on time on stream (TOS) model was used to analyze the experimental data. The simulated results were in good agreement with the experimental results, within an error less than ±5%. The estimated activation energies indicated that conversion of *m*-xylene to *p*-xylene in both acid-functionalized silicalite-1 membranes is affected by the mass transfer rate through the membrane, while conversion of *m*-xylene to *o*-xylene is controlled by the reaction rate.

1. Introduction

Para-xylene (*p*-xylene) is the feed for pure terephthalic acid (PTA) production which has the largest commercial market as compared to its isomers, meta-xylene (*m*-xylene) and ortho-xylene (*o*-xylene). With increasing demand of *p*-xylene, selective production of *p*-xylene by *m*-xylene isomerization using zeolite catalyst has gained considerable interest over the years and much attention has been focused on ZSM-5 zeolite as catalyst due to its high activity and shape selectivity [1,2]. Recently, the application of zeolite membrane as catalytic membrane has been reported by number of researchers [3–8] to improve *p*-xylene yield by selective removal of the product from the reactor. The application of catalytic membrane reactor has proven flexibility of its operation and improvement in product selectivity in Knoevenagel condensation reaction between benzaldehyde and ethyl acetoacetate [9–11].

van Dyk et al. [6] reported that *p*-xylene yield of about 10% was enhanced in an extractor-type membrane reactor as compare to the conventional fixed bed reactor. An increment in *p*-xylene production of 28% was observed by Tarditi et al. [5] using 100% exchanged Ba-ZSM-5 in the membrane reactor. Haag et al. [7] also reported 15% higher *m*-xylene conversion and 10% more *p*-xylene selectivity in H-ZSM-5 catalytic membrane reactor as compared to the conventional packed-bed reactor. Recently, Zhang et al. [8] reported that an increment of 26% *p*-xylene yield could be achieved in a silicalite-1 membrane reactor packed with H-ZSM-5 catalyst. However, H-ZSM-5 in membrane reactors gave moderate to low selectivity of *p*-xylene [12,13].

There is a need to develop a catalytic membrane in order to improve *p*-xylene yield, selectivity and separation rate. Due to the higher diffusion rate of *p*-xylene compared to *m*-xylene and *o*-xylene, *p*-xylene could be separated though silicalite-1 membrane [14–16]. However, silicalite-1 is catalytically inactive in its pure form (an aluminum-free analogue of ZSM-5 (Si/Al = ∞)). It is reported in the literature that selective and continuous removal of *p*-xylene from the reaction system could enhance xylene isomerization and thus higher selectivity and yield. Therefore, it has drawn an interest in the synthesis of silicalite-1 membrane with catalytic acid sites.

To best of our knowledge, synthesis of acid-functionalized silicalite-1 membrane and its performance in *m*-xylene isomerization has not been reported. Earlier, we reported the introduction of acid sites in silicalite-1, by adding organic-functional groups into the synthesis mixture and subsequent transformation of organic-functional group into acid-functionalized silicalite-1 [17]. The catalytic activity of these membranes in xylene isomerization

* Corresponding author. Tel.: +60 4 5996409; fax: +60 4 5941013.
E-mail address: chbhatia@eng.usm.my (S. Bhatia).

1385-8947/$ – see front matter © 2010 Elsevier B.V. All rights reserved.
doi:10.1016/j.cej.2010.01.022

Nomenclature

C_{exp}	experimental xylene concentration (mol m^{-3})
C_{sim}	simulated xylene concentration (mol m^{-3})
C_m	concentration of *m*-xylene (mol m^{-3})
C_p	concentration of *p*-xylene (mol m^{-3})
C_o	concentration of *o*-xylene (mol m^{-3})
E_i	activation energy (kJ/mol)
k_i	apparent rate constant (g^{-1} min^{-1})
k_o	frequency factor (min^{-1})
R	universal gas constant (8.314 J/mol K)
r_m	rate of reaction of *m*-xylene (mol m^{-3} min^{-1})
r_p	rate of reaction of *p*-xylene (mol m^{-3} min^{-1})
r_o	rate of reaction of *o*-xylene (mol m^{-3} min^{-1})
T	temperature (K)
t	time on stream (min)
τ	residence time (min)
W	membrane weight (g)

Greek letters

α	catalyst deactivation constant (min^{-1})

Subscripts

i	1, −1, 2, −2, 3, −3

Abbreviations

FT-IR	Fourier transform infrared spectroscopy
NH_3-TPD	ammonia temperature-programmed desorption
SEM	scanning electron microscope
m	meta
o	ortho
p	para
Y_{int}	initial guess of the parameter
Y_{new}	new value of the parameter

reaction has been reported in the present work. The kinetic parameters of the reaction needed for the design and scale up of catalytic membrane reactor has been obtained. Although the reaction scheme of xylene isomerization using acid catalysts has been reported by various researchers, there are still inconsistencies need to be addressed [2,18]. Therefore, suitable reaction scheme that can describe the catalytic activity of the acid-functionalized silicalite-1 membranes need to be figured out.

The objective of the present research is to study *m*-xylene isomerization using two types of catalytic silicalite-1 membranes namely: (i) propylsulfonic acid-functionalized silicalite-1 membrane and (ii) arenesulfonic acid-functionalized membrane. The membranes were synthesized, characterized and their activity in *m*-xylene isomerization reaction is investigated. A suitable kinetic model based on isomerization reaction scheme is proposed and kinetic parameters are obtained at different reaction temperature. The experimental results were compared with the simulated results obtained from the proposed model.

2. Experimental

2.1. Preparation of membranes

Acid-functionalized silicalite-1 membranes were synthesized on a porous α-alumina support by *in situ* hydrothermal crystallization method as reported in our previous work [16,17]. Firstly, a porous α-alumina support (diameter = 25 mm, thickness = 3 mm) was coated with a thin silica layer using sol–gel technique [19]. The role of the layer was to improve the structural stability and to reduce the mismatch between membrane and support during calcination [3]. The synthesis mixture was prepared by mixing tetrapropylammonium hydroxide (TPAOH, 1 M, Merck), double deionized water (DDI H_2O), tetraethylorthosilicate (TEOS, >98%, Merck) and organosilane source (OS) according to the molar composition:

$$5(1-x)\text{TEOS} : \text{TPAOH} : 1000\text{DDI}H_2O : 5x(\text{OS})$$

where x is molar ratio of the organosilane source, OS and $x = 0.10$. Two types of organosilane source, 3-mercaptopropyltrimethoxysilane (3MP) (85%, Acros) and phenethyltrimethoxysilane (PE) (>97%, Fluka) were the used in the present study, respectively. 4 g of TPAOH, 72 g of DDIH_2O, 3.6 g of TEOS and 0.34 g of 3MP were used for preparation of synthesis solution with 3MP molar ratio of 0.10, while 4 g of TPAOH, 72 g of DDIH_2O, 3.6 g of TEOS and 0.44 g of PE were needed for the preparation of synthesis solution with PE molar ratio of 0.10. The reaction mixture was stirred vigorously at room temperature, and then transferred into Teflon-lined vessel containing α-alumina support percoated with mesoporous silica layer. After hydrothermal crystallization for 1 day at 175 °C, the membrane was repeatedly washed with deionized water and dried at 100 °C overnight. In order to make sure that the membrane was fully coated on the support, nitrogen permeation test was performed on the membrane using permeability measurement before the removal of template [20]. The hydrothermal synthesis of the membrane was repeated until membrane was completely impermeable to nitrogen gas. Finally, the membrane was calcined at 420 °C for 15 h with a heating and cooling rate of 0.5 °C/min.

2.2. Post-synthesis modification

2.2.1. Silicalite-1 membrane with propylsulfonic acid sites

The thiol-functional group present in the membrane synthesized using 3MP was oxidized to propylsulfonic acid following the method reported by Zheng et al. [21]. The calcined membrane was placed inside a Teflon-lined vessel with the aid of a Teflon support holder where the membrane faced downward. The membrane was treated with 30% H_2O_2 (Merck) at room temperature for 24 h under stirring. After 24 h, the membrane was washed with DDI water and soaked in 0.1 M H_2SO_4 for 4 h. The membrane was again washed with DDI water and dried at 100 °C overnight.

2.2.2. Silicalite-1 membrane with arenesulfonic acid sites

The phenethyl-functional group present in the membrane synthesized using PE was sulfonated to arenesulfonic acid group following the method reported by Holmberg et al. [22]. The calcined membrane was dispersed in 96 wt% concentrated sulfuric acid and treated at 80 °C for 24 h under stirring. After 24 h, the membrane was washed extensively with DDI water and dried for overnight at 100 °C.

The membrane synthesized using 3MP is coded as MAFS-P10. Similarly, the membrane synthesized using PE is coded as MAFS-A10.

2.3. Characterization

The crystalline structure of the membranes was determined by XRD analysis using X-ray diffractometer (Philips PANanalytical X-Pert PRO) with CuK_α radiation ($\lambda = 1.5406$ Å) operated at 40 kV and 30 mA. The morphology and thickness of the membranes were determined using Zeiss Supra 35 VP scanning electron microscope (SEM) with W-Tungsten filament, operated at 3 kV. The acidity of acid-functionalized silicalite-1 samples was determined by temperature-programmed desorption of ammonia (NH_3-TPD)

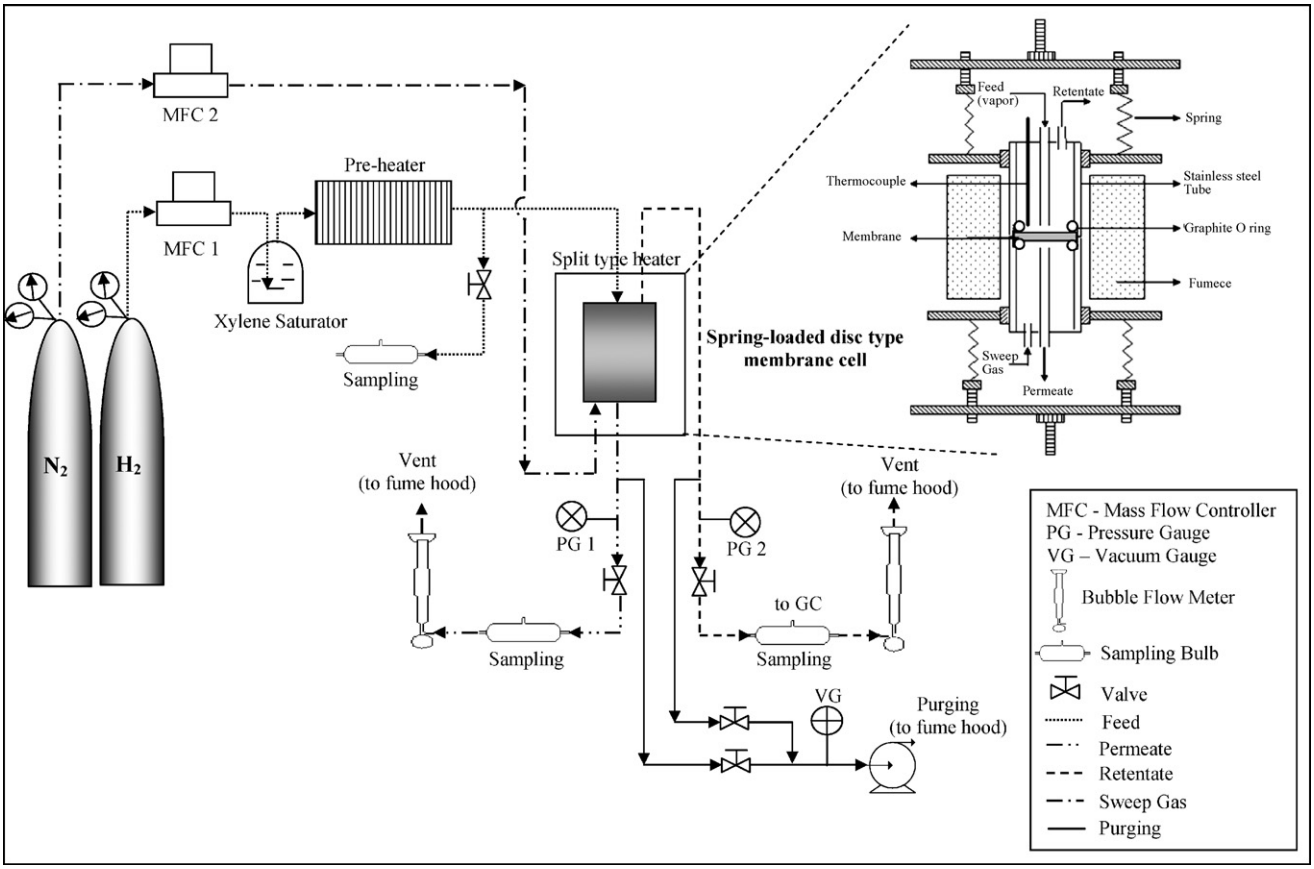

Fig. 1. Schematic of vapor permeation test rig for membrane separation and reaction in a single unit.

using Micromeritics AutoChem II 2920 V3.05 Chemisorp Analyzer. Approximately 0.02 g sample was pretreated in flowing helium (20 ml/min) at 200 °C for 1 h. After pretreatment, sample was cooled down to ambient in helium gas. Pulse chemisorption was performed to obtain acidity of sample by saturating the sample with 15% ammonia/helium. NH_3-TPD was carried out under a constant flow of helium (20 ml/min). The temperature was raised from ambient to 700 °C at a heating rate of 10 °C/min. The amount of ammonia desorbed was detected by a thermal conductivity detector (TCD) as desorption peak area. The nature of the acid sites of acid-functionalized silicalite-1 samples was determined using FT-IR technique. The IR spectra were recorded using a Perkin–Elmer FT-IR (Model 2000) in the range of 400–4000 cm^{-1} using KBr method. In order to determine the acid sites, prior to KBr method, the sample was first exposed to pyridine for 1 h; after degassing at 200 °C, followed by desorption of physically adsorbed of pyridine at 150 °C under vacuum.

2.4. Experimental setup for m-xylene isomerization study

Fig. 1 shows schematic of the experimental setup used for catalytic membrane reaction and separation in a single unit. The catalytic membrane disk was sealed with graphite O-rings in a custom-made spring-loaded type stainless steel reactor fixed inside a split type heater. The test rig consists of four sections: (a) feed, (b) preheating, (c) reaction and separation, and (d) product collection. Before start of the experiment, the catalytic membrane was pretreated at 200 °C under nitrogen flow for 3 h. The catalytic membrane side of the disk was fed with hydrogen gas passing through *m*-xylene (99+%, Acros) saturator maintained at 30 °C, while opposite membrane side was flushed with nitrogen gas as a sweep stream. The flow rates of the carrier and sweep gases were controlled with mass flow controllers (MKS Instruments). The weight hourly space velocity (WHSV) in the catalytic membrane reactor was adjusted by regulating the carrier flow through the saturator. In order to maintain the conversion below equilibrium and to avoid the formation of undesired products such as toluene or ethylbenzene, high weight hourly space velocity (WHSV) was used in the present study [5,6]. The WHSV for MAFS-P10 membrane was 1800 h^{-1}, corresponds to H_2 gas flow rate of 50 cm^3/min and *m*-xylene feed partial pressure of 0.94 kPa. For MAFS-A10 membrane, the WHSV was 1700 h^{-1}, corresponds to H_2 gas flow rate of 75 cm^3/min and *m*-xylene feed partial pressure of 1.56 kPa. The volumetric flow of the sweep gas was set at 20 cm^3/min. The total pressure at either sides of the catalytic membrane was maintained at 101 kPa. All system lines were kept at 180 °C using heating tape to prevent condensation of the xylene and to maintain correct xylene vapor pressure. The configuration of acid-functionalized silicalite-1 catalytic membrane reactor is shown in Fig. 2.

A Hewlett–Packard, Model 5890 series II gas chromatograph equipped with a Petrocol DH 50.2 capillary glass column (50 m long × 0.2 mm ID × film thickness 0.5 μm) and FID detector was

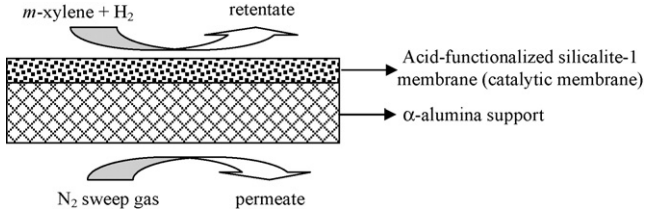

Fig. 2. Catalytic membrane reactor configuration for *m*-xylene isomerization reaction and *p*-xylene separation in a single unit.

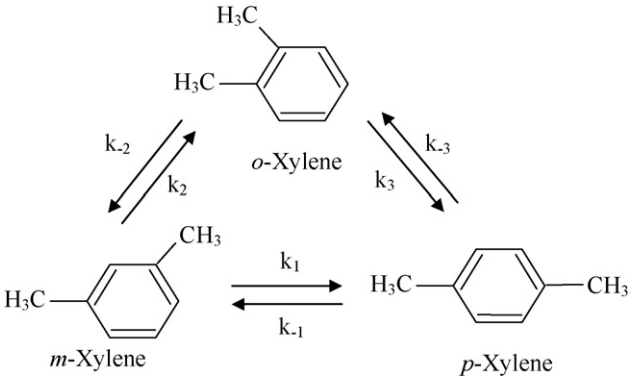

Fig. 3. Triangular reaction scheme of xylene isomerization.

used to analyze the feed, permeate and retentate streams. The *m*-xylene conversion, *p*-xylene yield, *o*-xylene yield and *p*-xylene selectivity are defined as follows:

$$m\text{-xylene conversion}\,(\%) = \frac{\text{moles of } m\text{-xylene converted}}{\text{moles of } m\text{-xylene in the feed}} \times 100 \quad (1)$$

$$p\text{-xylene yield}\,(\%) = \frac{\text{moles of } p\text{-xylene in products (permeate + retentate)}}{\text{moles of } m\text{-xylene in the feed}} \times 100 \quad (2)$$

$$o\text{-xylene yield}\,(\%) = \frac{\text{moles of } o\text{-xylene in products (permeate + retentate)}}{\text{moles of } m\text{-xylene converted}} \times 100 \quad (3)$$

$$p\text{-xylene selectivity}\,(\%) = \frac{\text{moles of } p\text{-xylene in products (permeate + retentate)}}{\text{moles of } m\text{-xylene converted}} \times 100 \quad (4)$$

The volumetric flow rates of the retentate and permeate streams were measured at atmospheric pressure and room temperature using bubble flowmeter. The catalytic membrane area available for xylene reaction and separation was 2.00×10^{-4} m^2.

3. Kinetic modeling

In the literature, two different reaction schemes are reported to describe xylene isomerization (by ignoring disproportionation reaction): (1) a general triangular scheme for the three xylenes and (2) a simple linear scheme in which the reaction is assumed to proceed via intramolecular 1,2-shifts of the methyl groups. The latter allows transformation of *o*- into *p*-xylene (and vice versa) only through *m*-xylene as an intermediate step, but not directly [7]. Both schemes have been used by different researchers for the xylene isomerization reaction using zeolite catalyst [2,18,23–26].

In the present work, a suitable kinetic model to represent *m*-xylene isomerization using acid-functionalized silicalite-1 membrane as catalyst is proposed. Since the yield of *p*-xylene and *o*-xylene were underestimated using linear scheme, therefore, triangular reaction scheme was adopted in the present study. Fig. 3 shows the triangular reaction scheme of xylene isomerization. The catalytic membrane reactor is assumed to be operated under isothermal condition and membrane weight is taken equivalent to the catalyst weight.

The differential equations describing the kinetics of *m*-xylene isomerization are assumed to be first order with respect to the reactant [7,18] based on the triangular reaction scheme. The rate of reaction is assumed to be proportional to the amount of catalyst [1,7,27]:

$$r_m = \frac{dC_m}{d\tau} = -[(k_1 + k_2)C_m - k_{-1}C_p - k_{-2}C_o] \times W \times \exp(\alpha t) \quad (5)$$

$$r_p = \frac{dC_p}{d\tau} = -[(k_{-1} + k_{-3})C_p - k_1 C_m - k_3 C_o] \times W \times \exp(\alpha t) \quad (6)$$

$$r_o = \frac{dC_o}{d\tau} = -[(k_{-2} + k_3)C_o - k_2 C_m - k_{-3} C_p] \times W \times \exp(\alpha t) \quad (7)$$

where r_m, r_p and r_o represent rate of reaction (mol m^{-3} min^{-1}) of *m*-xylene, *p*-xylene or *o*-xylene, respectively. C_m, C_p and C_o represent concentration (mol m^{-3}) of *m*-xylene, *p*-xylene or *o*-xylene, respectively, and W represents the catalytic membrane weight (g). τ represents residence time (min) and t represents time on stream (min). k_i represents apparent rate constant (g^{-1} min^{-1}), while α (min^{-1}) applied in the models as catalyst deactivation constant. The temperature dependence of the apparent rate constant is represented as follows:

$$k_i = k_o \exp\left[-\frac{E_i}{RT}\right] \quad (8)$$

Seven parameters of $k_1, k_2, k_3, k_{-1}, k_{-2}, k_{-3}$ and α were estimated by solving Eqs. (5)–(7) using ordinary differential equation (ODE) solver available in POLYMATH (Version 5.1). The solution routine start with an initial guess of k_1, k_2, k_3, k_{-1}, k_{-2}, k_{-3} and α. The initial guess of these parameters was made by referring to the data reported in the literature [1,2,7]. The best fit was verified by evaluating the simulated and experimental C_m, C_p and C_o which should be in close agreement with the convergence less than ±0.05. If the difference between simulated and experimental values was more than ±0.05, the new value of the parameter is calculated as follows:

$$Y_{new} = Y_{int} \pm (0.05\, Y_{int}) \quad (9)$$

where Y_{new} is new value of the parameter and Y_{int} represents initial guess of the parameter. The new value will be used to solve the equations and new simulated concentration values are compared with the experimental values. This process continues till the convergence is reached within an acceptable error (±0.05). Fig. 4

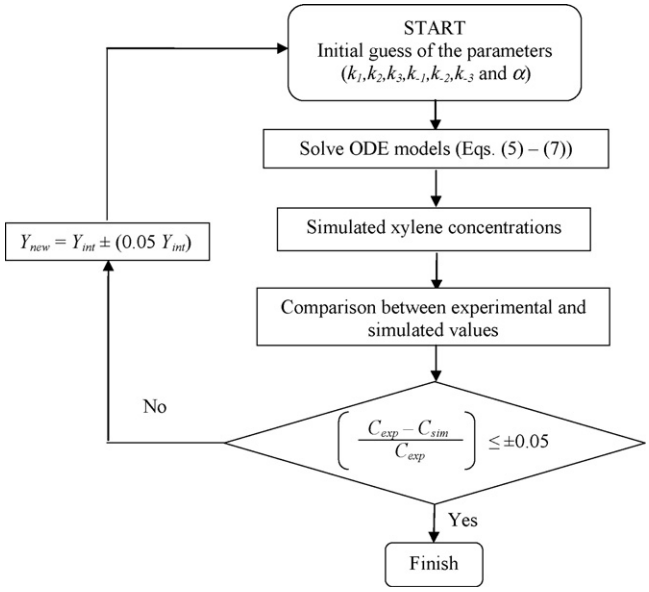

Fig. 4. Flow chart algorithm of the solution procedure.

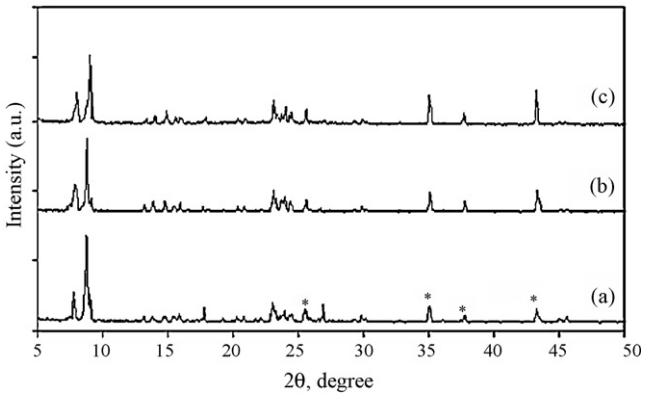

Fig. 5. XRD patterns of (a) silicalite-1 [17], (b) MAFS-P10 and (c) MAFS- A10. *Peak coming from α-alumina support.

shows the flow chart of the solution procedure followed to obtain the kinetic parameters.

4. Results and discussion

4.1. Membrane crystallinity and surface morphology by XRD and SEM

Fig. 5 shows XRD patterns of the membranes. Fig. 5a shows XRD pattern of parent silicalite-1 membrane reported in our previous work [16]. Propylsulfonic acid-functionalized silicalite-1 membrane (MAFS-P10) (Fig. 5b) exhibited diffraction patterns similar to that of silicalite-1 membrane but with different crystallinity. The degree of crystallinity was indicated by the peak intensity, which represent the crystalline phase in the membranes. The crystallinity of the membrane was calculated as follows [17]:

$$\%\text{XRD crystallinity} = \frac{\text{Sum of peak intensities of the sample}}{\text{Sum of peak intensities of the reference}} \times 100 \quad (10)$$

by considering three strong peaks at $2\theta \sim 7.7^\circ$, 8.8° and 23°, and silicalite-1 membrane reported in our previous work [16] was used as reference.

The crystallinity of the MAFS-P10 was 69% (MAFS-P10). XRD pattern of arenesulfonic acid-functionalized silicalite-1 membrane (MAFS-A10) (Fig. 5c) also exhibited diffraction patterns similar to that of silicalite-1 membrane, the peak intensity of MAFS-A10 was slightly lower than that of peak intensity of MAFS-P10. The relative crystallinity of MAFS-A10 obtained was 63%. These results show that the acid-functionalized membrane became partially crystalline, with the presence of amorphous phases. The differences in crystallinity of both acid-functionalized silicalite-1 membranes could be due to the molecular weight of the organosilane sources. PE has higher molecular weight compared to 3MP. This resulted in higher disruption of the crystal structure, due to more difficult for PE to incorporate into the sample structure compared to 3MP, and thus, causing reduction in membrane crystallinity.

Fig. 6 shows SEM micrographs of acid-functionalized silicalite-1 membranes and both crystalline and amorphous phases were observed in the membranes. Although coffin shape of silicalite-1 was retained and the crystal size was reduced compared to the size of silicalite-1 crystal on silicalite-1 membrane as reported in

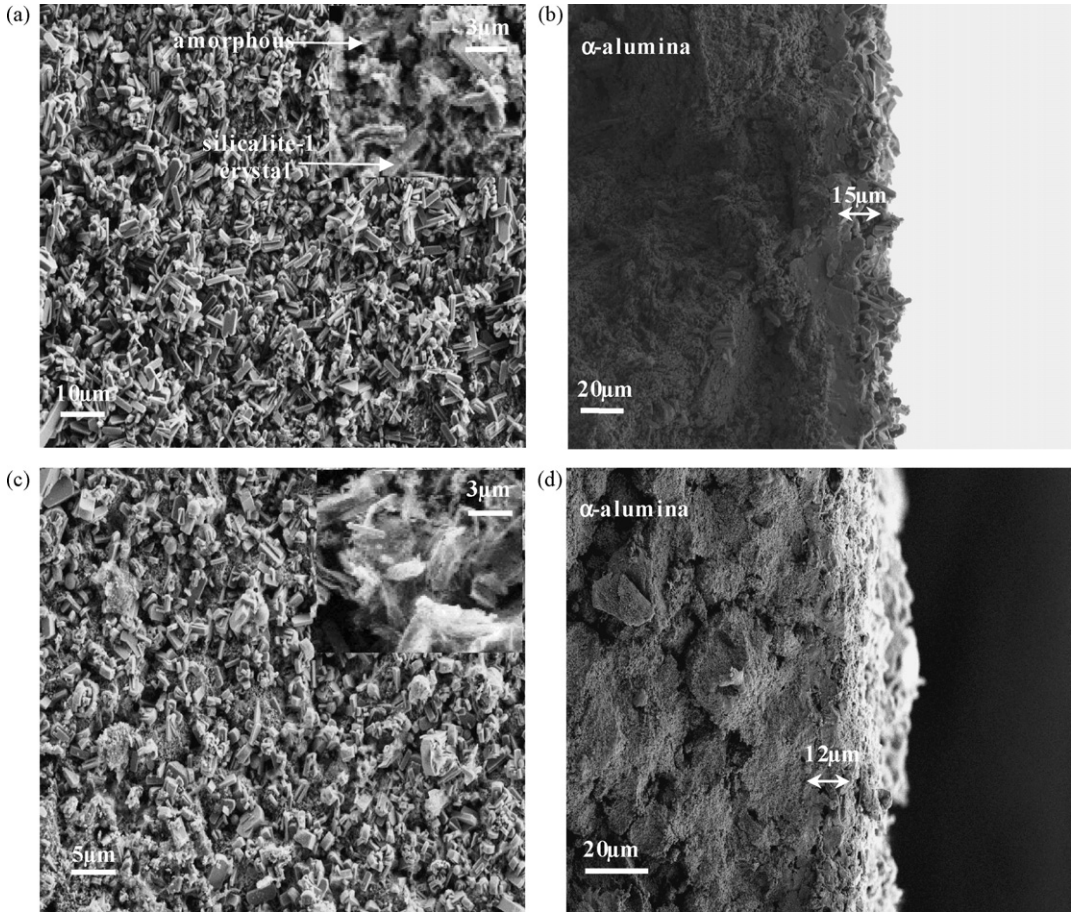

Fig. 6. SEM surface morphology of (a) MAFS-P10, (c) MAFS-A10 membranes and cross-section view of (b) MAFS-P10 and (d) MAFS-A10 membranes.

Table 1
Weight and thickness of acid-functionalized silicalite-1 membranes.

Membrane	Gain in weight after preparation (g)	Membrane thickness from SEM (μm)	Membrane weight for reaction according to membrane area (g)
MAFS-P10	0.0723	15	0.0493
MAFS-A10	0.0933	12	0.0636

Table 2
Estimation of acidity from NH_3-TPD on acid-functionalized silicalite-1 samples.

Sample	Weak acid site 150 °C (mmol H^+/g)	Medium acid site 280–350 °C (mmol H^+/g)	Strong acid site 550 °C (mmol H^+/g)	[a]Total acidity (mmol H^+/g)
AFS-P10	0.00	0.34	1.20	1.54
AFS-A10	0.23	0.60	1.69	2.52

[a] Determined from pulse chemisorption.

our previous study [16]. This shows that silicalite-1 crystals in the acid-functionalized silicalite-1 membranes are partially crystalline [17]. Arenesulfonic acid-functionalized silicalite-1 membrane (MAFS-A10, Fig. 6b) exhibits similar morphology as propylsulfonic acid-functionalized silicalite-1 membrane (MAFS-P10, Fig. 6a), but with the presence of higher amorphous phase and smaller silicalite-1 crystal size. The higher molecular weight of PE compared to 3MP resulted in higher disruption of the crystal structure, and thus, resulting in higher amorphous phases. This observation was in agreement with the results obtained from XRD.

The thickness and weight of acid-functionalized silicalite-1 membranes are presented in Table 1. The thickness of membranes was measured from the cross-section of SEM micrographs. In order to obtain a representative estimate of membrane thickness, the average thickness was measured at three different points. As shown in cross-section SEM micrographs (Fig. 6b and d), a continuous, and dense layer was observed. Due to the presence of higher amorphous phase and smaller silicalite-1 crystal, MAFS-A10 membrane is thinner as compared to MAFS-P10 membrane. The membrane thickness was 15 μm for MAFS-P10 and 12 μm for MAFS-A10, respectively. From Table 1, it is noted that MAFS-A10 membrane had more weight than that of MAFS-P10. This was due to higher molecular weight of PE (the presence of aromatic ring) and increased the membrane weight.

4.2. Acidity and nature of acid sites by NH_3-TPD and FT-IR

The NH_3-TPD and FT-IR analyses of both acid-functionalized silicalite-1 were carried using powder sample obtained from the bottom of the Teflon-lined vessel during synthesis of membranes. Silicalite-1 sample obtained in previous study [16] was also characterized for NH_3-TPD and FT-IR in order to compare the nature and locations of acid sites between acid-functionalized silicalite-1 and silicalite-1 samples.

The distribution of surface acidity and strength of acid sites of acid-functionalized silicalite-1 samples was determined by ammonia temperature-programmed desorption (NH_3-TPD). NH_3-TPD profile for the samples is shown in Fig. 7. It is noted that three adsorption peaks were observed in propylsulfonic acid-functionalized silicalite-1 sample (AFS-P10, Fig. 7b). The peak before 100 °C was attributed to the physically adsorbed NH_3 [28], and other two desorption peaks in the range of 300–400 and 500–600 °C represent medium and strong acid strength, respectively. As compared with propylsulfonic acid-functionalized silicalite-1 sample, extra desorption peak at 130–200 °C was observed in NH_3-TPD profile of arenesulfonic acid-functionalized silicalite-1 sample (AFS-A10, Fig. 7c). Total four adsorption peaks in the temperature range of 50–100 °C (physically adsorbed NH_3), 130–200 °C (weak acid sites), 200–330 °C (medium acid sites) and 500–600 °C (strong acid sites) were obtained in arenesulfonic acid-functionalized silicalite-1 sample. Table 2 shows the quantitative estimation of acid sites and strength distribution of the samples obtained from the area under adsorption peaks. The total acidity and strength of acid sites of AFS-A10 was higher than that of AFS-P10, as also indicated by the higher intensity of desorption peak in NH_3-TPD profile. The higher acid capacity of AFS-A10 could be due to the presence of aromatic ring, which increased the sample acidity after strong acid treatment. NH_3-TPD profile parent silicalite-1 only shows one desorption peak at temperature below 100 °C (Fig. 7a), which indicates that acid sites were not present in silicalite-1 sample.

The nature of acid sites present in the samples was analyzed from FT-IR spectra. Fig. 8 shows FT-IR spectra of pyridine adsorbed on acid-functionalized silicalite-1 and silicalite-1 samples. IR spectra show adsorption peaks at 1638 and 1542 cm^{-1}, corresponds to strong Brönsted acid sites for both samples [29]. The weak absorbances at 1420 and 1470 cm^{-1} for AFS-P10 (Fig. 8b) were assigned to the bending vibrations of methylene groups, CH_2 [30]. The peak at 1490 cm^{-1} was observed in AFS-A10 (Fig. 8c), corresponds to pyridine adsorbed on both Lewis and Brönsted acid sites [31]. Silicalite-1 did not show the presence of acid sites as shown in Fig. 8a, which is consistent with NH_3-TPD profile. Based on the results obtained from NH_3-TPD and FT-IR, the acid sites of both acid-functionalized silicalite-1 samples were mostly located in amorphous phases of the samples.

4.3. m-Xylene isomerization in acid-functionalized silicalite-1 catalytic membrane reactor

The results of *m*-xylene isomerization using acid-functionalized silicalite-1 membranes at various reaction temperatures are shown

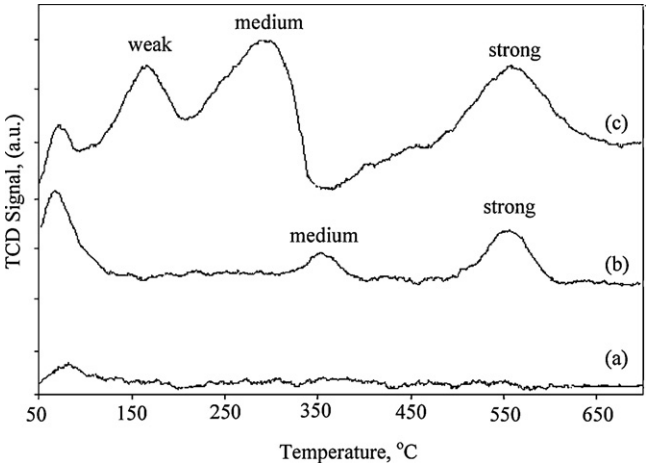

Fig. 7. NH_3-TPD profile for (a) silicalite-1 [13], (b) AFS-P10 and (c) AFS-A10.

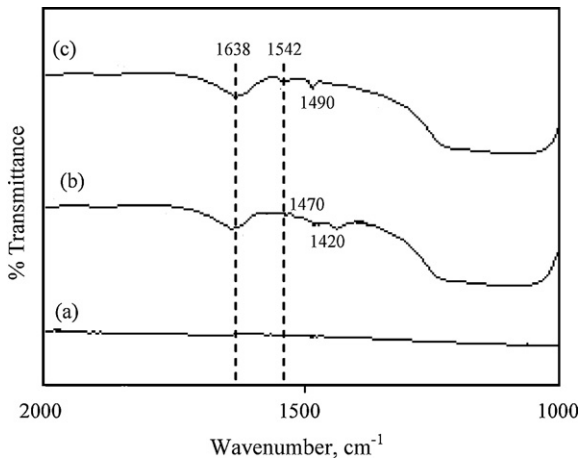

Fig. 8. FT-IR spectra of pyridine adsorbed on (a) silicalite-1 [14], (b) AFS-P10 and (c) AFS-A10.

in Fig. 9. It was observed that with increase in reaction temperature increased *m*-xylene conversion, *p*-xylene selectivity and *p*-xylene yield. *m*-Xylene conversion over MAFS-A10 membrane was 42.5%, 47.7% and 52% at reaction temperature of 355, 400 and 450 °C, respectively. As the reaction temperature increased from 355 to 450 °C, *p*-xylene selectivity increased from 58.8% to 62.6%, while *p*-xylene yield increased from 25.0% to 31.7%.

MAFS-P10 membrane showed similar trend of *m*-xylene isomerization results as obtained over MAFS-A10 membrane, but with lower catalytic activity. *m*-xylene conversion of 31.2% was obtained at 355 °C, and increased to 40.6% at 450 °C, while *p*-xylene selectivity increased from 55.9% to 59.4% as the reaction temperature increased from 355 to 450 °C. MAFS-P10 membrane gave *p*-xylene yield of 17.5%, 21.1% and 24.2% at reaction temperature of 355, 400 and 450 °C, respectively.

Between two types of catalytic membranes studied, MAFS-A10 membrane performed better and gave higher *m*-xylene conversion, *p*-xylene yield and *p*-xylene selectivity. It is well documented in the literature that *m*-xylene isomerization through intramolecular mechanism is catalyzed by strong Brönsted acid sites [13,32]. FT-IR and NH_3-TPD results shows that MAFS-A10 membrane has higher acidity as compared to MAFS-P10 membrane, although strong Brönsted acid sites are present in both catalytic membranes (Table 2).

m-Xylene conversion and *p*-xylene yield obtained were higher in the present study using arenesulfonic acid-functionalized silicalite-1 membrane as compared to other types of catalytic membranes reported in the literature [5–8]. The acid density and continuous removal of the reaction products are the important factors and contributed to the improvement of *m*-xylene isomerization activity. Fig. 10 shows *p*-xylene flux over MAFS-P10 and MAFS-A10 membrane as a function of temperature. The temperature dependence of *p*-xylene flux was due to increase in *p*-xylene concentration in the reaction zone, causing higher diffusion rate of *p*-xylene through the membrane with increase in temperature.

The *p*-xylene flux obtained over MAFS-A10 membrane was higher than that of MAFS-P10 membrane. At reaction temperature of 355 °C, *p*-xylene flux of 3.74×10^{-6} mol/m^2 s was obtained in MAFS-A10 membrane. As the temperature increased from 400 to 450 °C, the *p*-xylene flux increased from 3.98×10^{-6} to 5.11×10^{-6} mol/m^2 s. These results show that the presence of higher amount of amorphous phase and smaller silicalite-1 crystals improved diffusitivity of *p*-xylene through the membrane. Zhang et al. [8] reported that *p*-xylene flux of 2.40×10^{-6} mol/m^2 s was obtained (silicalite-1 membrane reactor packed with H-ZSM-5 catalyst) at reaction temperature of 330 °C, which was lower than the flux value obtained in the present work. The present study shows that higher *p*-xylene selectivity and yield over arenesulfonic acid-functionalized silicalite-1 membrane is attributed to more effective removal of *p*-xylene through membrane. The continuous separation of the reaction products through membrane enhanced *m*-xylene isomerization activity.

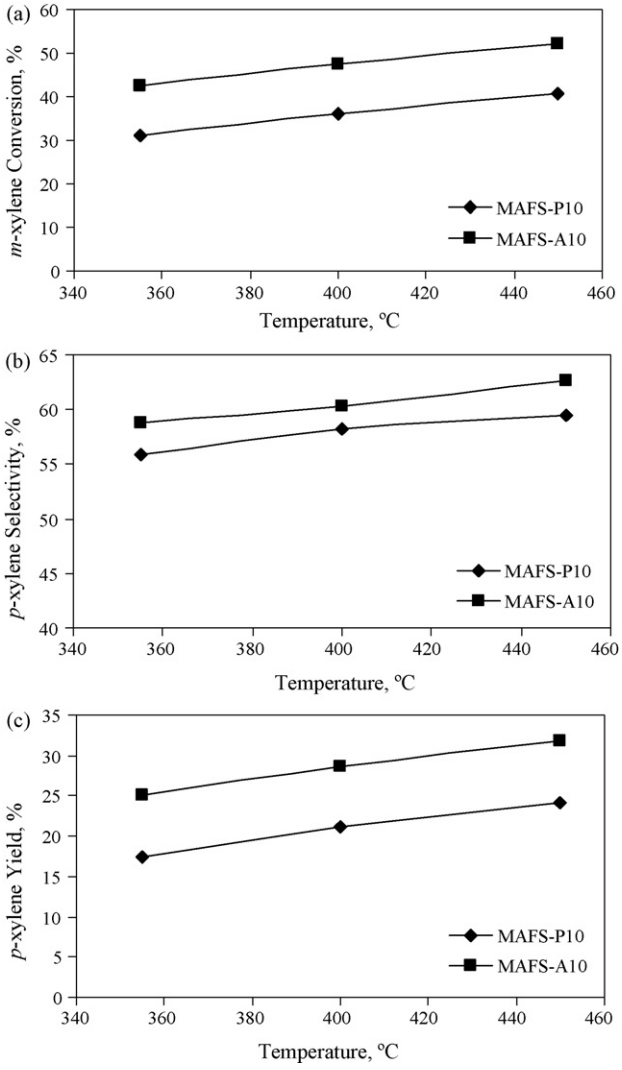

Fig. 9. Isomerization results in MAFS-P10 and MAFS-A10 catalytic membrane reactors as a function of temperature.

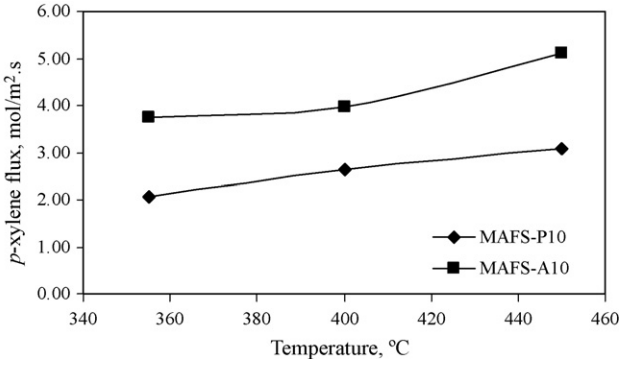

Fig. 10. *p*-Xylene flux over MAFS-P10 and MAFS-A10 catalytic membrane reactors as a function of temperature.

Table 3
Estimated kinetic parameters for *m*-xylene isomerization based on time on stream (TOS) using propylsulfonic acid-functionalized silicalite-1 catalytic membrane (MAFS-P10).

Temperature (°C)	k_1 (g^{-1} min^{-1})	k_2 (g^{-1} min^{-1})	k (g^{-1} min^{-1})	k_{-1} (g^{-1} min^{-1})	k_{-2} (g^{-1} min^{-1})	k_{-3} (g^{-1} min^{-1})	α (min^{-1})
355	0.168	0.029	0.054	0.460	0.015	0.051	0.020
400	0.215	0.041	0.079	0.608	0.021	0.083	0.030
450	0.258	0.057	0.096	0.703	0.031	0.097	0.030
k_o (min^{-1})	4.450	4.970	4.467	11.914	3.710	7.268	
E_i (kJ/mol)	17.060	26.853	22.905	16.883	28.830	25.6221	

Table 4
Estimated kinetic parameters for *m*-xylene isomerization based on time on stream (TOS) using arenesulfonic acid-functionalized silicalite-1 catalytic membrane (MAFS-A10).

Temperature (°C)	k_1 (g^{-1} min^{-1})	k_2 (g^{-1} min^{-1})	k_3 (g^{-1} min^{-1})	k_{-1} (g^{-1} min^{-1})	k_{-2} (g^{-1} min^{-1})	k_{-3} (g^{-1} min^{-1})	α (min^{-1})
355	0.691	0.035	0.088	1.451	0.016	0.093	0.020
400	0.837	0.047	0.113	1.672	0.021	0.112	0.030
450	0.989	0.063	0.141	1.870	0.031	0.168	0.035
k_o (min^{-1})	10.623	3.062	3.195	10.099	2.390	7.983	
E (kJ/mol)	14.252	23.354	18.737	10.113	26.251	23.445	

Both of the membranes were stable and gave reproducible catalytic activity after experimental runs for 120 h of operation at temperature ranged from 355 to 450 °C. The presence of higher amount of amorphous phase in MAFS-A10 did not affect the catalytic stability of the membrane. The membrane performed well in *m*-xylene isomerization and separation of *p*-xylene from its isomers although some voids between individual crystals were observed. This could be due to the presence of compact intermediate layer under the top layer.

4.4. m-Xylene isomerization kinetics modeling

4.4.1. Kinetic parameters

The apparent kinetic parameters for *m*-xylene isomerization over MAFS-P10 and MAFS-A10 membranes at different reaction temperatures are presented in Tables 3 and 4, respectively. The frequency factor and activation energy were calculated using Arrhenius relationship (Eq. (8)) and the plot of ln *k* as a function of reciprocal of temperature is shown in Figs. 11 and 12, respectively.

It can be observed in Tables 3 and 4, k_{-1} has the largest value among the apparent rate constants with its smallest activation energy, E_{-1}. This indicates that conversion of *p*-xylene to *m*-xylene (k_{-1}) was the easiest on the catalytic membranes. E_{-1} was slightly less than E_1, shows that the conversion of *p*-xylene to *m*-xylene was slightly easier than that of conversion of *m*-xylene to *p*-xylene (k_1). E_{-1} and E_1 obtained over MAFS-P10 membrane were slightly higher than 15 kJ/mol indicates that conversion of *p*-xylene to *m*-xylene (k_{-1}) and *m*-xylene to *p*-xylene (k_1) falls in the transition regime of diffusion and chemical reaction [2]. However, acidity of the membrane and reaction conditions remained constant throughout the experiments. Therefore, the rate of diffusion of xylene isomers through the membrane is more important compared to the chemical reaction for conversions of *p*-xylene to *m*-xylene (k_{-1}) and vice versa (k_1). E_{-1} and E_1 obtained over MAFS-A10 membrane (Table 4) were lower than 15 kJ/mol. This implies that conversions of *p*-xylene to *m*-xylene (k_{-1}) and *m*-xylene to *p*-xylene (k_1) in MAFS-A10 membrane are controlled by diffusional rate.

The activation energies of E_2, E_{-2}, E_3 and E_{-3} were higher than that of E_1 and E_{-1} (Tables 3 and 4), show that apparent reaction rate constants of k_2, k_{-2}, k_3 and k_{-3} are controlled by chemical reaction in the membrane [2]. It is reported that isomerization of xylene is an acid-catalyzed reaction and the extent of interaction between acidic site and adsorbed species would depend on acid strength of the site and basicity of individual molecule [2]. Based on the magnitude of activation energies, E_{-2} exhibited highest value followed by E_2 (Tables 3 and 4). This implies that it is more difficult to cause the shift of methyl group in aromatic ring, from *o*-xylene to *m*-xylene, or from *m*-xylene to *o*-xylene in the catalytic membranes. Therefore, chemical reaction plays an important role for conversions of *m*-xylene to *o*-xylene and vice versa. The results obtained in the present study suggested that the adsorption strength of xylene isomers on both catalytic membranes is in the order of *o*-xylene > *m*-xylene ≫ *p*-xylene, in line with the results reported by Li et al. [2] using H-ZSM-5 zeolite catalyst. Besides, xylene isomerization results show that quantity of *p*-xylene in products exceeds that of *o*-xylene, mainly due to *o*-xylene would undergo further isomerization before diffusing from the membrane.

It can be observed that apparent reaction rate constants, k_{-1}, k_1, k_2, k_{-2}, k_3, and k_{-3} obtained using MAFS-A10 membrane (Table 4)

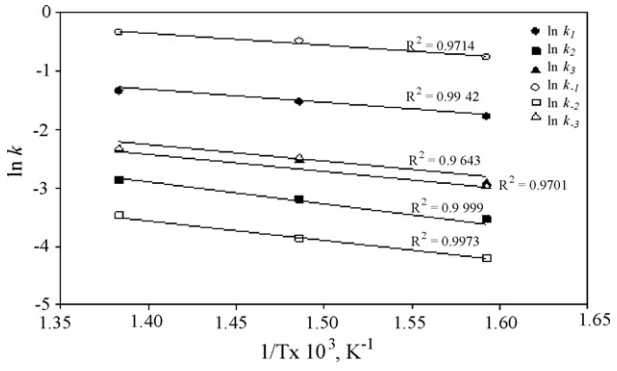

Fig. 11. Apparent reaction rate constant, *k* as a function of reciprocal of temperature, 1/*T* for *m*-xylene isomerization using propylsulfonic acid-functionalized silicalite-1 catalytic membrane reactor (MAFS-P10).

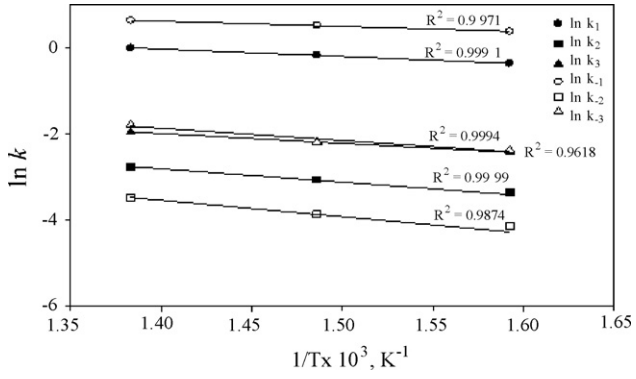

Fig. 12. Apparent reaction rate constant, *k* as a function of reciprocal of temperature, 1/T for *m*-xylene isomerization over arenesulfonic acid-functionalized silicalite-1 catalytic membrane reactor (MAFS-A10).

Table 5
Comparison between experimental and simulated *m*-xylene conversion in acid-functionalized silicalite-1 catalytic membrane reactor.

Time (min)	MAFS-P10 membrane Temperature (°C)						MAFS-A10 membrane Temperature (°C)					
	355		400		450		355		400		450	
	Exp.	Sim.	Exp.	Sim.	Exp.	Sim.	Exp.	Sim.	Exp.	Sim.	Exp.	Sim.
10	13.03	13.17	14.25	13.61	11.15	11.48	27.71	27.83	30.50	29.98	34.88	33.47
20	20.83	19.98	25.15	24.13	21.83	22.04	32.26	31.15	36.02	35.73	39.46	38.40
30	27.90	26.60	28.00	28.69	27.45	27.77	37.67	36.72	39.71	38.93	42.38	41.41
40	28.87	27.59	31.75	32.65	33.83	32.78	41.11	41.42	42.53	42.28	45.61	44.55
50	31.03	29.90	34.84	34.44	39.75	37.77	42.60	42.00	46.28	45.17	50.30	49.14
60	31.24	30.14	35.87	34.82	40.23	39.02	42.73	42.92	47.04	46.97	52.17	50.53
Mean error (%)	3.20		1.22		0.99		0.96		1.27		2.80	
Standard deviation	2.14		3.20		3.80		1.77		2.92		0.70	

were higher than that of those values obtained using MAFS-P10 membrane (Table 3). This was due to the presence of higher concentration of strong acid sites and total acid sites in MAFS-A10 membrane (Table 2) [32]. The activation energies, E_i obtained using MAFS-A10 membrane were lower than that of E_i obtained using MAFS-P10 membrane, and thus, better isomerization activity is observed over MAFS-A10 membrane. The higher value of apparent rate constants k_1 indicated that conversion of *m*-xylene to *p*-xylene was relatively faster over MAFS-A10 membrane as compared to MAFS-P10 membrane. Therefore, higher *p*-xylene yield was obtained (Fig. 9c). The difference in activation energy shows that there was a difference in the catalyst intrinsic acidity of the active sites between these two membranes, which is consistent with NH_3-TPD (Fig. 7) and FT-IR results (Fig. 8), respectively.

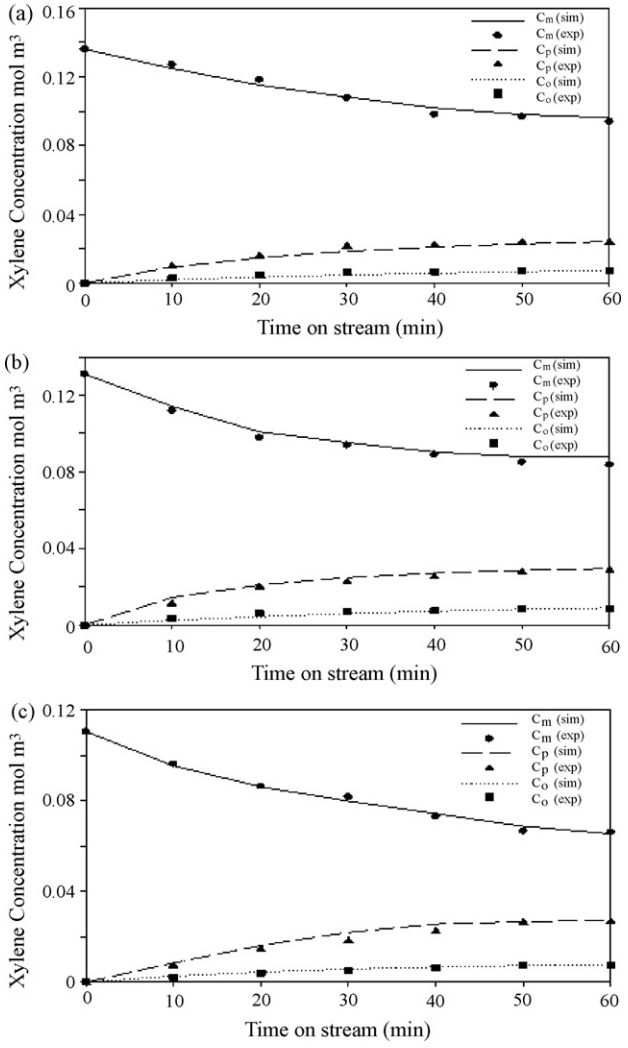

Fig. 13. Comparison between experimental and simulated data for *m*-xylene isomerization in propylsulfonic acid-functionalized silicalite-1 (MAFS-P10) catalytic membrane reactor: (a) 355 °C, (b) 400 °C and (c) 450 °C.

Since *m*-xylene isomerization is well represented by triangular reaction scheme, these results confirmed that acidity (chemical reaction) and continuous removal of reaction products (diffusion rate) through membrane are the important factors contributed to *m*-xylene isomerization activity in acid-functionalized silicalite-1 membranes. The catalyst deactivation constant, α for both membranes is slightly changed with increase in the reaction temperature (Tables 3 and 4). This indicates that during isomerization, some of the acid sites could be covered with the intermediates and thus did not participate in the reaction. However, α value was relatively small and did not affect the overall membrane performance in the isomerization reaction.

4.4.2. Comparison between simulated and experimental results

The comparison between simulated and experimental results of *m*-xylene isomerization using MAFS-P10 and MAFS-A10 membranes at various reaction temperatures is shown in Figs. 13 and 14, respectively. Tables 5 and 6 compare simulated *m*-xylene conversion and *p*-xylene yield with the experimental results. It can be observed that the simulated results are in good agreement with the experimental results within an error less than ± 5%. A normal distribution of residuals with regression coefficient of 0.999 was observed in the reconciliation plots of *p*-xylene selectivity as shown in Fig. 15. These results indicate that triangular reaction scheme based on time on stream (TOS) models (Eqs. (5)–(7)) is appropriate for *m*-xylene isomerization reaction over acid-functionalized silicalite-1 membrane as catalytic membrane.

4.5. Comparison with the literature results

Kinetic studies for *m*-xylene isomerization using catalytic membrane reactor are only reported by Haag et al. [7] using H-ZSM-5 membrane. Table 7 compares the activation energies obtained in this work with the reported activation energies by Haag et al. [7]. It can be observed that activation energies obtained in the present study were lower than that of those values reported by Haag et al. [7]. This could be due to (a) higher *p*-xylene flux; (b) structure and morphology and (c) higher acid capacity of acid-functionalized silicalite-1 membrane. The continuous removal of the reaction products through membrane increased the *p*-xylene yield.

Table 6
Comparison between experimental and simulated *p*-xylene yield in acid-functionalized silicalite-1 catalytic membrane reactor.

Time, min	MAFS-P10 membrane Temperature (°C)						MAFS-A10 membrane Temperature (°C)					
	355		400		450		355		400		450	
	Exp.	Sim.	Exp.	Sim.	Exp.	Sim.	Exp.	Sim.	Exp.	Sim.	Exp.	Sim.
10	7.36	7.00	8.34	8.57	6.69	7.02	15.84	16.05	18.60	18.93	21.22	22.40
20	11.76	11.22	14.72	15.19	13.10	13.70	18.44	19.33	21.96	22.47	24.01	25.62
30	15.75	15.18	16.39	17.05	16.48	17.23	21.54	20.82	24.20	24.81	25.78	26.32
40	16.30	15.84	18.58	19.25	20.31	20.88	23.51	23.80	25.97	25.69	27.75	28.17
50	17.52	16.75	20.39	21.37	23.86	24.10	24.35	25.20	28.25	29.64	30.60	29.88
60	17.46	17.74	21.12	22.05	24.15	24.69	25.01	25.24	28.59	29.67	31.74	31.57
Mean error (%)	3.10		−3.80		−3.36		−1.41		−2.38		−2.17	
Standard deviation	2.43		0.77		1.59		2.78		2.03		3.48	

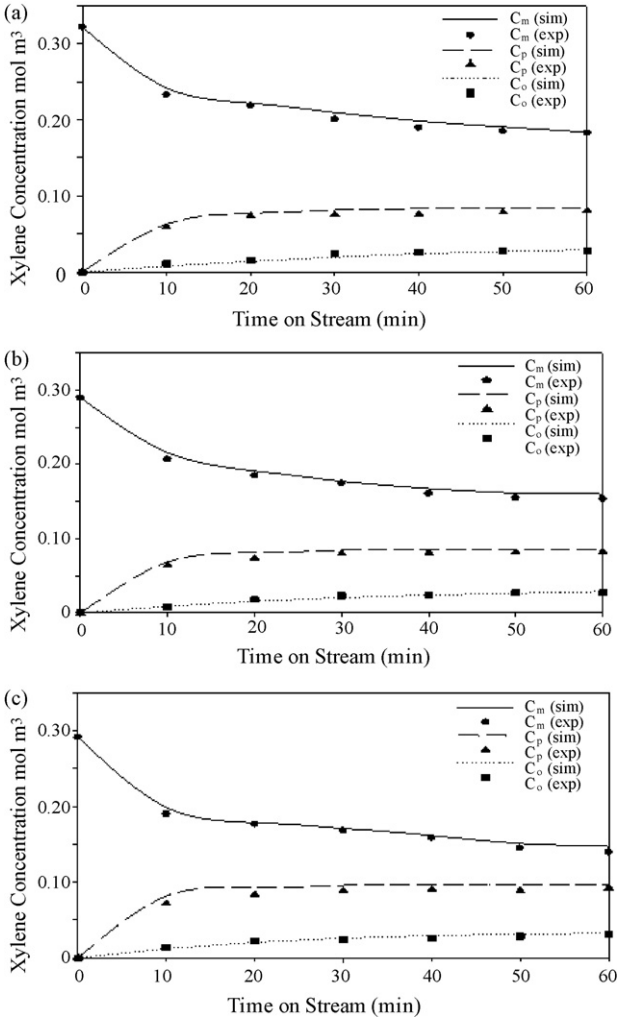

Fig. 14. Comparison between experimental and simulated data for *m*-xylene isomerization in arenesulfonic acid-functionalized silicalite-1 (MAFS-A10) catalytic membrane reactor: (a) 355 °C, (b) 400 °C and (c) 450 °C.

Table 7
Comparison of the activation energies obtained in the present work and literature.

Catalytic membrane	Activation energies, E_i (kJ/mol)						Ref.
	E_1	E_2	E_3	E_{-1}	E_{-2}	E_{-3}	
H-ZSM-5	36.3	56.6	39.8	35.8	32.9	35.9	[7]
MAFS-P10	17.1	26.9	22.9	16.9	28.8	25.6	Present study
MAFS-A10	14.3	23.4	18.7	10.1	26.3	23.4	Present study

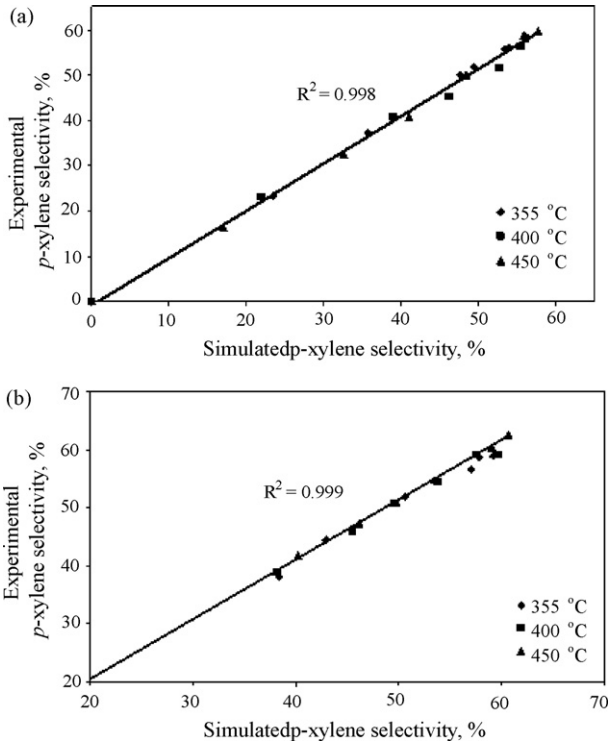

Fig. 15. Comparison between experimental and simulated values for *p*-xylene selectivity, %. (a) MAFS-P10 and (b) MAFS-A10 catalytic membrane reactors.

5. Conclusion

In the present study, propylsulfonic and arenesulfonic acid-functionalized silicalite-1 catalytic membranes were synthesized using 10 mol% of 3-mercaptopropyltrimethoxysilane (3MP) and 10 mol% of phenethyltrimethoxysilane (PE) as an organosilane sources, respectively. SEM micrographs show that well intergrowth membranes were formed. NH_3-TPD and FT-IR studies show that strong Brönsted acid sites were present in both acid-functionalized silicalite-1membranes. The membranes were tested for *m*-xylene isomerization at reaction temperature from 355 to 450 °C and the results were adequately analyzed by triangular reaction scheme. The experimental results show that arenesulfonic acid-functionalized silicalite-1 membrane performed better in *m*-xylene isomerization reaction as compared to propylsulfonic acid-functionalized silicalite-1 membrane, with *m*-xylene conversion of 52% and *p*-xylene yield of 32% at reaction temperature of 450 °C.

The kinetic parameters determined using triangular reaction scheme indicated that *m*-xylene isomerization reaction rates in

both membranes were affected by the diffusional mass transfer rates. The enhancement in *m*-xylene conversion and *p*-xylene yield using arenesulfonic acid-functionalized silicalite-1 membrane as compared to propylsulfonic acid-functionalized silicalite-1 membrane was due to its lower activation energies and presence of higher acidity. The kinetic parameters reported in the present study will be useful in the rational deign of catalytic membrane reactor for the production of *p*-xylene through xylene isomerization.

Acknowledgements

The financial support provided by Ministry of Science, Technology and Innovation (MOSTI) under e-Science Fund Grant (Account No. 6013319), Ministry of Higher Education under FRGS (Account No. 6070021) and Research University Grant (Account No. 811043) from Universiti Sains Malaysia (USM) are duly acknowledged.

References

[1] S. Al-Khattaf, Enhancing *p*-xylene selectivity during *m*-xylene transformation using mildly pre-coked ZSM-5 catalyst, Chem. Eng. Process. 46 (2007) 964–974.
[2] Y. Li, X. Chang, Z. Zeng, Kinetics study of the isomerization of xylene on HZSM-5 zeolite. 1. Kinetics model and reaction mechanism, Ind. Eng. Chem. Res. 31 (1992) 187–192.
[3] G. Saracco, H.W.J.P. Neomagus, G.F. Versteeg, W.P.M. van Swaaij, High-temperature membrane reactors: potential and problems, Chem. Eng. Sci. 54 (1999) 1997–2017.
[4] J. Coronas, J. Santamaría, Catalytic reactors based on porous ceramic membranes, Catal. Today 51 (1999) 377–389.
[5] A.M. Tarditi, G.I. Horowitz, E.A. Lombardo, Xylene isomerization in a ZSM-5/SS membrane reactor, Catal. Lett. 123 (2008) 7–15.
[6] L. van Dyk, L. Lorenzen, S. Miachon, J.A. Dalmon, Xylene isomerization in an extractor type catalytic membrane reactor, Catal. Today 104 (2005) 274–280.
[7] S. Haag, M. Hanebuth, G.T.P. Mabande, A. Avhale, W. Schwieger, R. Dittmeyer, On the use of a catalytic H-ZSM-5 membrane for xylene isomerization, Micropor. Mesopor. Mater. 96 (2006) 168–176.
[8] C. Zhang, Z. Hong, X. Gu, Z. Zhong, W. Jin, N. Xu, Silicalite-1 zeolite membrane reactor packed with HZSM-5 catalyst for meta-xylene isomerization, Ind. Eng. Chem. Res. 48 (2009) 4293–4299.
[9] S.M. Lai, R. Martin-Aranda, K.L. Yeung, Knoevenagel condensation reaction in a membrane microreactor, Chem. Commun. 2 (2003) 218–219.
[10] S.M. Lai, C.P. Ng, R. Martin-Aranda, K.L. Yeung, Knoevenagel condensation reaction in zeolite membrane microreactor, Micropor. Mesopor. Mater. 66 (2003) 239–252.
[11] W.N. Lau, K.L. Yeung, R. Martin-Aranda, Knoevenagel condensation reaction between benzaldehyde and ethyl acetoacetate in microreactor and membrane microreactor, Micropor. Mesopor. Mater. 115 (2008) 156–163.
[12] J.-H. Kim, T. Kunieda, M. Niwa, Generation of shape-selectivity of *p*-xylene formation in the synthesized ZSM-5 zeolites, J. Catal. 173 (1998) 433–439.
[13] S. Zheng, A. Jentys, J.A. Lercher, Xylene isomerization with surface-modified HZSM-5 zeolite catalysts: an in situ IR study, J. Catal. 241 (2006) 304–311.
[14] Z. Lai, G. Bonilla, I. Diaz, J.G. Nery, K. Sujaoti, M.A. Amat, E. Kokkoli, O. Terasaki, R.W. Thompson, M. Tsapatsis, D.G. Vlachos, Microstructural optimization of a zeolite membrane for organic vapor separation, Science 300 (2003) 456–460.
[15] G. Xomeritakis, Z. Lai, M. Tsapatsis, Separation of xylene isomer vapors with oriented MFI membranes made by seeded growth, Ind. Eng. Chem. Res. 40 (2001) 544–552.
[16] Y.F. Yeong, A.Z. Abdullah, A.L. Ahmad, S. Bhatia, Process optimization studies of *p*-xylene separation from binary xylene mixture over silicalite-1 membrane using response surface methodology, J. Membr. Sci. 341 (2009) 96–108.
[17] Y.F. Yeong, A.Z. Abdullah, A.L. Ahmad, S. Bhatia, Synthesis, structure and acid characteristics of partially crystalline silicalite-1 based materials, Micropor. Mesopor. Mater. 123 (2009) 129–139.
[18] A. Iliyas, S. Al-Khattaf, Gas phase isomerization of meta-xylene over USY zeolite in a riser simulator: a simplified kinetic model, Chem. Eng. J. 107 (2005) 127–132.
[19] G. Xomeritakis, S. Naik, C.M. Braunbarth, C.J. Cornelius, R. Pardey, C.J. Brinker, Organic-templated silica membranes. I. Gas and vapor transport properties, J. Membr. Sci. 215 (2003) 225–233.
[20] M. Torres, M. Gutiérrez, L. López, V. Múgica, R. Gomez, J.A. Montoya, Controlled crystal growth of β zeolite films on alumina supports, Mater. Lett. 62 (2008) 1071–1073.
[21] Y. Zheng, X. Su, X. Zhang, W. Wei, Y. Sun, Functionalized mesoporous SBA-15 silica with propylsulfonic groups as catalysts for esterification of salicylic acid with dimethyl carbonate, Stud. Surf. Sci. Catal. 156 (2005) 205–212.
[22] B.A. Holmberg, S.J. Hwang, M.E. Davis, Y. Yan, Synthesis and proton conductivity of sulfonic acid functionalized zeolite BEA nanocrystals, Micropor. Mesopor. Mater. 80 (2005) 347–356.
[23] A. Corma, F. Llopis, J.B. Monton, Influence of the structural parameters of Y zeolite on the transalkylation of alkylaromatics, J. Catal. 140 (1993) 384–394.
[24] S. Bhatia, S. Chandra, T. Das, Simulation of the xylene isomerization catalytic reactor, Ind. Eng. Chem. Res. 28 (1989) 1185–1190.
[25] Y.S. Hsu, T.Y. Lee, H.C. Hu, Isomerization of ethylbenzene and *m*-xylene on zeolites, Ind. Eng. Chem. Res. 27 (1988) 942–947.
[26] O. Cappellazzo, G. Cao, G. Messina, M. Morbidelli, Kinetics of shape-selective xylene isomerization over a ZSM-5 catalyst, Ind. Eng. Chem. Res. 30 (1991) 2280–2287.
[27] M. Minceva, P. Sa Gomes, V. Meshko, A.E. Rodrigues, Simulated moving bed reactor for isomerization and separation of *p*-xylene, Chem. Eng. J. 140 (2008) 305–323.
[28] G. Yang, J. He, Y. Yoneyama, Y. Tan, Y. Han, N. Tsubaki, Preparation, characterization and reaction performance of H-ZSM-5/cobalt/silica capsule catalysts with different sizes for direct synthesis of isoparaffin, Appl. Catal. A: Gen. 329 (2007) 99–105.
[29] Y.S. Ooi, S. Bhatia, Aluminum-containing SBA-15 as cracking catalyst for the production of biofuel from waste used palm oil, Micropor. Mesopor. Mater. 102 (2007) 310–317.
[30] X. Wang, S. Cheng, J.C.C. Chan, Propylsulfonic acid-functionalized mesoporous silica synthesized by in situ oxidation of thiol groups under template-free condition, J. Phys. Chem. C 111 (2007) 2156–2164.
[31] V. Vishwanathan, K.W. Jun, J.W. Kim, H.S. Roh, Vapour phase dehydration of crude methanol to dimethyl ether over Na-modified H-ZSM-5 catalysts, Appl. Catal. A: Gen. 276 (2004) 251–255.
[32] Y. Li, H. Jun, Kinetic study of the isomerization of xylene on ZSM-5 zeolites: the effect of the modification with MgO and CaO, Appl. Catal. A: Gen. 142 (1996) 123–137.